Electronic Supplementary Information:

Sculpting the Shapes of Giant Unilamellar Vesicles using Isotropic-Nematic-Isotropic Phase Cycles

Purvil Jani[a], Karthik Nayani[b] and Nicholas L. Abbott*[a]

[a]School of Chemical and Biomolecular Engineering, Cornell University, Ithaca, NY, USA.
[b]Department of Chemical Engineering, University of Arkansas, Fayetteville, AR, USA.
*Corresponding author. Email: nabbott@cornell.edu

1. Observations of Tubules

As shown in Fig. S1, a GUV formed in DSCG solution (15% w/w) by the method of gentle hydration is strained in the nematic phase at 25 °C (Fig. S1 A). Upon decreasing the temperature of the sample to 20°C, the GUV was observed to form tubules from the two poles of the strained shape (Fig. S1 B).
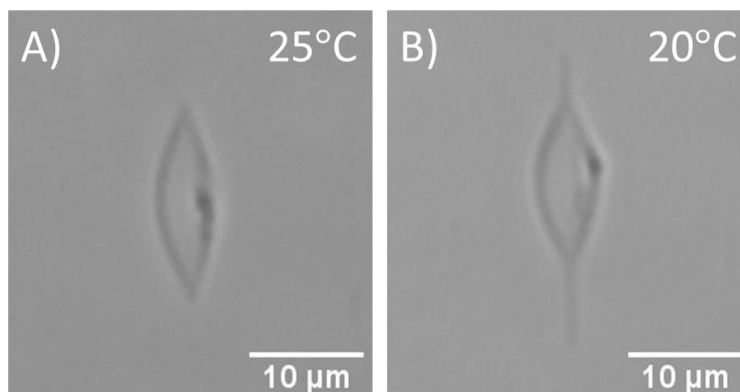

Fig. S1. Bright-field micrographs of a GUV in nematic phase of DSCG (15% w/w) at (A) 25°C, showing a spindle-like shape and (B) at 20°C, showing the formation of tubules from the poles of the strained GUV.

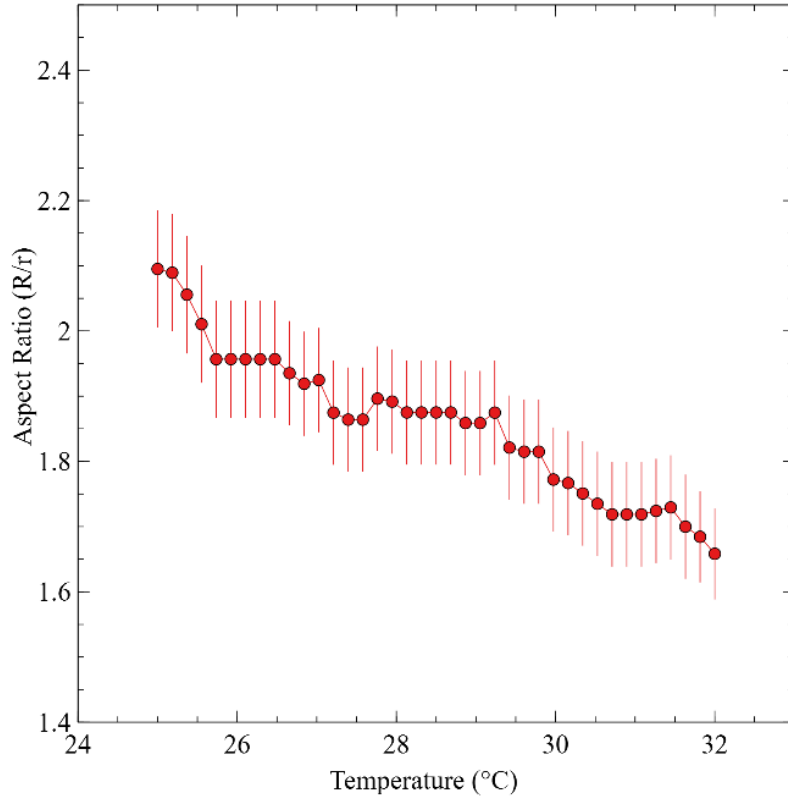## 2. Change of GUV aspect ratio with temperature in nematic DSCG

Fig. S2. Plot of aspect ratio (R/r) with temperature of a single GUV in the nematic phase of DSCG (15% (wt/wt)) (the error bars represent uncertainty in measuring the length of axes of the GUV from their micrographs)

3. Energy scaling in N+I phase

The observation of a strained GUV shape with a nematic interior indicates that the shapes of these GUVs continue to be determined by the interplay of the interfacial surface energy (of the interface between GUV surface and the nematic domain), E_S, and the elastic deformation energy, E_{LC}, of the nematic LC domain. The bending energy of the GUV membrane, E_B, is negligible in comparison to E_S and E_{LC} (see Eq. 2). For the nematic phase present only on one side of the membrane, we expect that E_{LC} will decrease compared to when LC is present on both sides of the membrane. Moreover, in this two phase region, the length of DSCG aggregates is decreased [1] (compared to the N phase), hence, we suspect that E_S (which, as noted above, is thought to arise from the depletion of DSCG aggregates near the GUV membrane [2]) will also decrease. Overall, however, we predict that the scaling of the

energetic contributions to the free energy of the GUV in the N phase will be similar to the N+I phase, namely

$$E_S \propto \tau R^2 \approx 10^4 - 10^6 \text{ pN nm,} \qquad \text{[Eq. 2 (a)]}$$

$$E_{LC} \propto KR \approx 10^4 - 10^5 \text{ pN nm,} \qquad \text{[Eq. 2 (b)]}$$

$$E_B \propto B \approx 10 - 40 \text{ pN nm,} \qquad \text{[Eq. 2 (c)]}$$

where τ is the interfacial tension between the GUV surface and the nematic LC phase ($\tau \sim 0.01 \text{ mN/m}$ [2]), K is the average elastic constant of the LC (10 pN for 15% w/w DSCG [3]) and B is the bending stiffness of DOPC membranes [4] (a function of elastic modulus and membrane geometry).

4. INI cycle of a single GUV

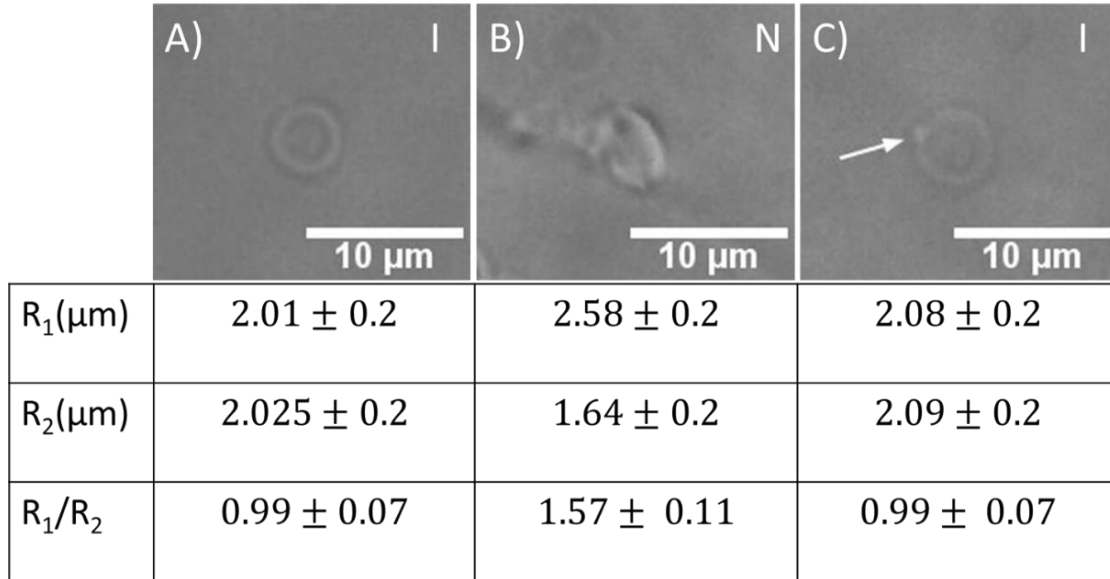|	A)	B)	C)
R_1(μm)	2.01 ± 0.2	2.58 ± 0.2	2.08 ± 0.2
R_2(μm)	2.025 ± 0.2	1.64 ± 0.2	2.09 ± 0.2
R_1/R_2	0.99 ± 0.07	1.57 ± 0.11	0.99 ± 0.07

Fig. S3. Bright-field micrographs of a single GUV prepared by the method of electroformation in DSCG solution of 17% w/w concentration, undergoing an INI cycle. (A) Initial spherical shape of the GUV in the isotropic phase at 48°C (B) Strained shape of the same GUV in the nematic phase at 25°C. (C) The GUV regains its spherical shape upon heating the sample again to the isotropic phase (48°C), with the addition of a bud (indicated by an arrow). The table below the images shows corresponding values of radii of the GUV, measured in orthogonal directions (for (B) the orthogonal directions are along the major and minor axes of the strained GUV). (The error bars represent uncertainty in measuring the length of axes of the GUV from their micrographs).

5. Calculation of Δa and v

The lengths of semi-major (R) and semi-minor (r) axes of the strained shapes of GUVs are measured using an image processing software (ImageJ). Surface area (SA) and volume (V) of highly strained GUVs are calculated from the expressions shown below, evaluated by considering the GUV to be a body of revolution of parabolic curves.

$$SA = \frac{\pi}{16r^2}[2r(8r^2 - R^2)\sqrt{4r^2 + R^2} + (16r^2R^2 + R^4)\sinh^{-1}(\tfrac{2r}{R})] \qquad \text{[Eq. S1]}$$

$$V = \frac{16}{15}\pi Rr^2 \qquad \text{[Eq. S2]}$$

The reduced quantities, Δa and v, are then calculated using the following expressions. Here, D is the bilayer thickness, assumed to be 2 nm.

$$\Delta a \equiv \frac{\Delta A}{8\pi DR_0} \qquad \text{[Eq. S3]}$$

$$v \equiv \frac{V}{\left(\frac{4\pi}{3}\right)R_0^3} \qquad \text{[Eq. S4]}$$

Where

$$\Delta A = SA(R^{out}, r^{out}) - SA(R^{in}, r^{in}) \qquad \text{[Eq. S4]}$$

and

$$R_0 = \left(\frac{SA}{4\pi}\right)^{\frac{1}{2}} \quad ; R^{out}, R^{in} = R + \frac{D}{2}, R - \frac{D}{2}; r^{out}, r^{in} = r + \frac{D}{2}, r - \frac{D}{2} \quad \text{[Eq. S5 (a), (b), (c)]}$$

4
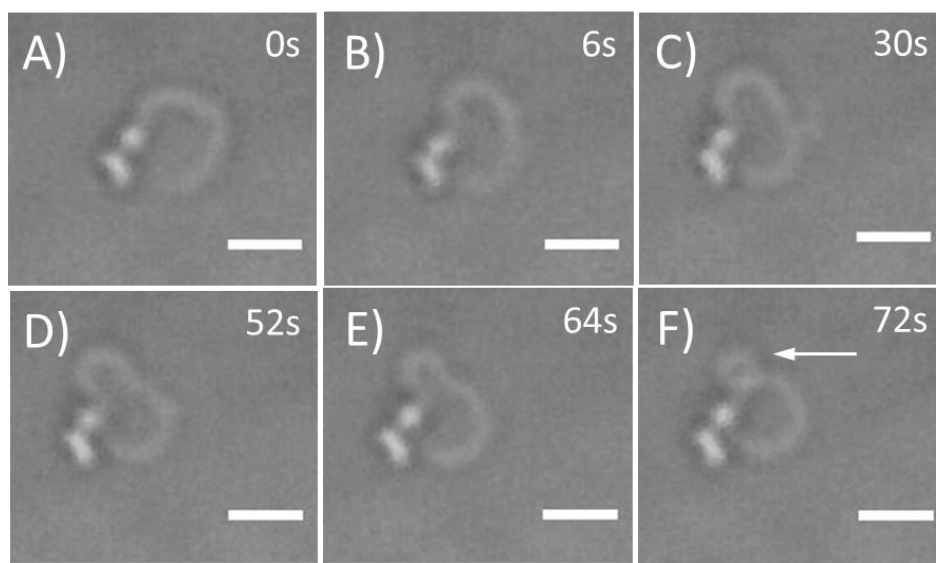
6. Formation of secondary structures

Fig. S4. (A-F) Bright-field micrographs of a GUV shedding excess membrane after complete transition to the isotropic phase, over a time-period of ~72s (numbers indicate timestamps with time = 0s at complete phase transition). (Scale bars: 5 μm). (F) Arrow indicates the location of the bud.

The experimental procedures reported in this study enabled us to make additional observations regarding the shapes of GUVs, including the formation of a secondary structure after the N→I transition. Fig. S4 shows images of a GUV (formed by the method of gentle hydration, in DSCG of 15% w/w concentration, at 48°C) in the I phase after undergoing an INI cycle, forming a bud (daughter vesicle). We observed the GUV to adopt an equilibrium shape over a time period of ~72s. Upon a complete transition to the isotropic phase, the GUV rearranges its membrane to initially form a pear shape (Fig. S4 C-E). The GUV then continuously transforms towards a limiting pear shape (where the neck connecting the parent GUV to the bud narrows) and finally forms a budded vesicle (Fig. S4 F).

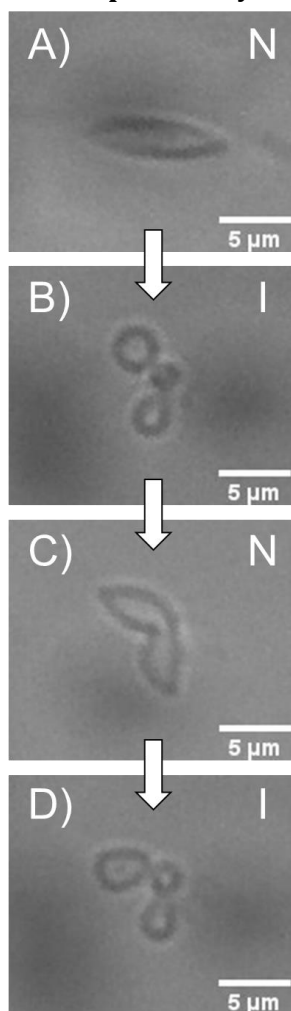## 7. Additional observations based on multiple I-N-I cycles

Fig. S5. Bright-field micrographs of a GUV undergoing cycling with temperature changing from (A) 25°C (nematic phase) to (B) 48°C (isotropic phase) to (C) 25°C (nematic phase) and back to (D) 48°C (isotropic phase). [Values of

As shown in Fig. S5, a GUV (formed in DSCG 15% w/w, by the method of gentle hydration) was strained repeatedly with LC elastic forces. The GUV was observed to adopt a spindle-like shape in the nematic phase (25°C) (Fig. S5 A). Upon heating the sample to the isotropic phase (48°C), the GUV was observed to form buds (Fig. S5 B). This budded GUV was observed to form a single strained vesicle (Fig. S5 C) upon cooling down the sample to the nematic phase (25°C) (the appearance of the GUV suggests that it adhered to the surface of the sample cell, thus perturbing the strained shape). Upon heating the sample again to the isotropic phase (48°C) we observed the GUV to form buds (Fig. S5 D).

This observation further supports our conclusion that budded GUVs do not physically separate and are parts of a single assembly.

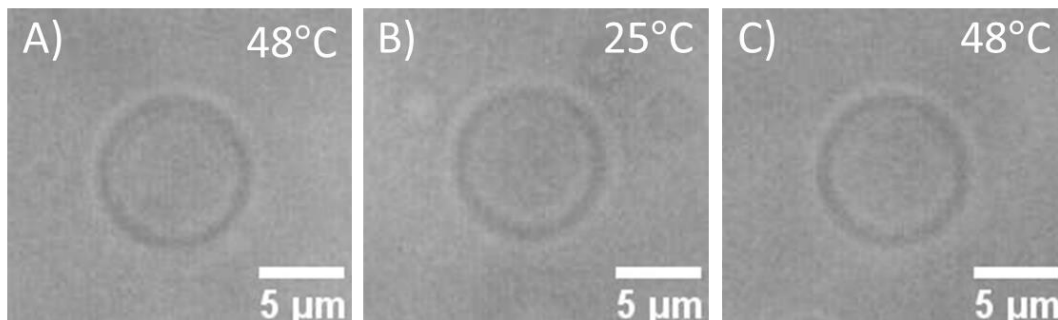## 8. Temperature cycling in absence of LC elastic forces

Fig. S6. Bright-field micrographs of a GUV prepared in DSCG solution (5% w/w) undergoing a change in temperature from (A) 48°C to (B) 25°C to (C) 48°C

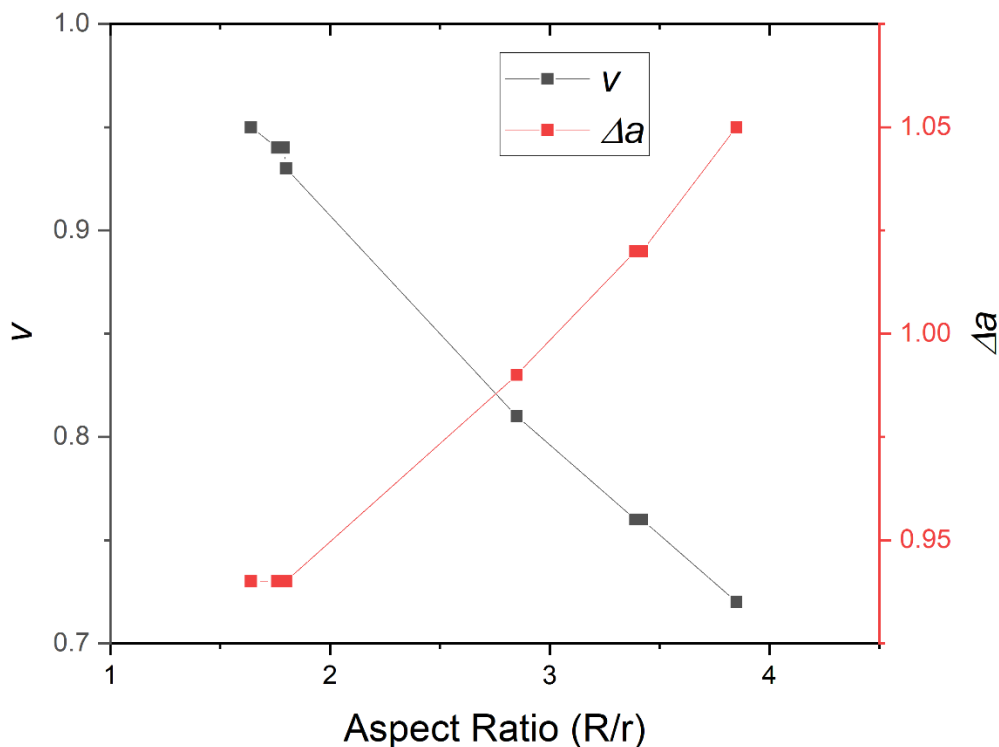## 9. Dependence of *Δa* and *v* on aspect ratio (R/r)

Fig. S7. Plot of experimentally measured values of aspect ratio (R/r), reduced volume (*v*) and reduced area (*Δa*) for GUVs strained in nematic DSCG solutions.
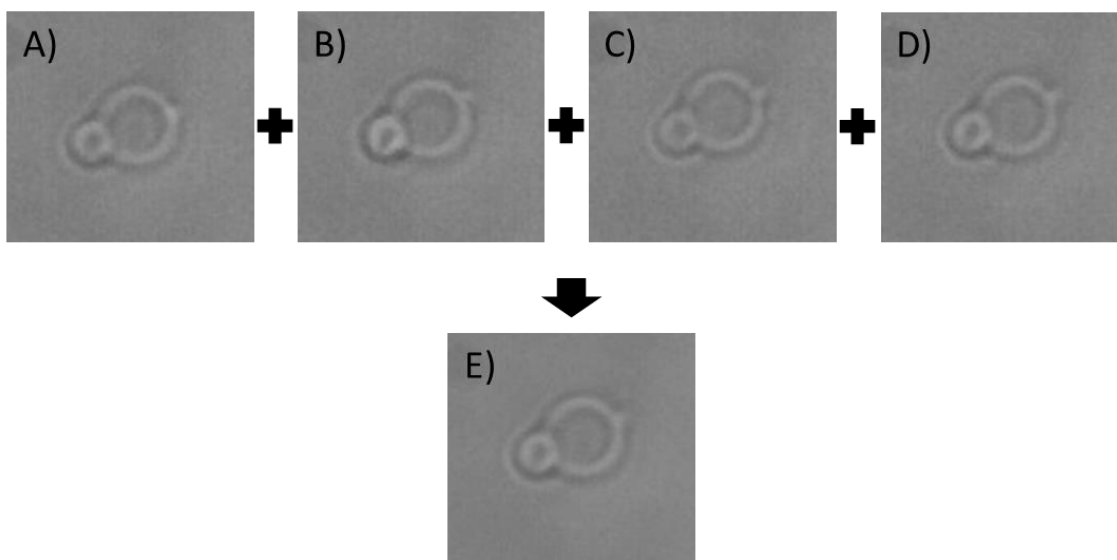
10. Image enhancement

Fig. S8. (A-E) Bright-field micrographs of a GUV in the isotropic phase. (A-D) Raw images are combined to obtain (E) an average image

As shown in Fig. S8, images of GUVs in the isotropic phase were enhanced by combining raw images. For the images of GUVs in the isotropic phase shown in Fig. 4 and Fig. 5, up to 10 raw images of each GUV were aligned with the GUV in center and then averaged (using the software ImageJ) to obtain a final image. We observed the averaged images to have less background noise and enhanced appearance of the GUVs when compared to raw images.

References

1. J. Lydon, *J. Mater. Chem.*, 2010, **20**, 10071-10099.
2. P. C. Mushenheim, J. S. Pendery, D. B. Weibel, S. E. Spagnolie and N. L. Abbott, *Proc Natl Acad Sci U S A*, 2016, **113**, 5564-5569.
3. S. Zhou, K. Neupane, Y. A. Nastishin, A. R. Baldwin, S. V. Shiyanovskii, O. D. Lavrentovich and S. Sprunt, *Soft Matter*, 2014, **10**, 6571-6581.
4. G. Niggemann, M. Kummrow and W. Helfrich, *J Phys Ii*, 1995, **5**, 413-425.